

HIGH PRESSURE/TEMPERATURE METAL SILICATE PARTITIONING OF TUNGSTEN. G.A. Shofner¹, L. Danielson², K. Richter², and A.J. Campbell¹, ¹Univ. of Maryland, Dept. of Geology, College Park, MD 20742, gshofner@umd.edu, ajc@umd.edu, ²NASA-JSC, Houston, TX 77058, lisa.r.danielson@nasa.gov, kevin.richter-1@nasa.gov.

Introduction: The behavior of chemical elements during metal/silicate segregation and their resulting distribution in Earth's mantle and core provide insight into core formation processes. Experimental determination of partition coefficients allows calculations of element distributions that can be compared to accepted values of element abundances in the silicate (mantle) and metallic (core) portions of the Earth^{1,2}.

Tungsten (W) is a moderately siderophile element and thus preferentially partitions into metal versus silicate under many planetary conditions². The partitioning behavior has been shown to vary with temperature, silicate composition, oxygen fugacity, and pressure. Most of the previous work on W partitioning has been conducted at 1-bar conditions or at relatively low pressures, i.e. ≤ 10 GPa^{3,4,5,6}, and in two cases at or near 20 GPa^{7,8}. According to those data, the stronger influences on the distribution coefficient of W are temperature, composition, and oxygen fugacity with a relatively slight influence in pressure. Predictions based on extrapolation of existing data and parameterizations suggest an increased pressure dependence on metal/silicate partitioning of W at higher pressures⁵. However, the dependence on pressure is not as well constrained as T, fO_2 , and silicate composition. This poses a problem because proposed equilibration pressures for core formation range from 27 to 50 GPa, falling well outside the experimental range, therefore requiring extrapolation of a parameterized model^{5, 8, 9, 10}. Higher pressure data are needed to improve our understanding of W partitioning at these more extreme conditions.

Experiments: We measured the partitioning behavior of W in high pressure and temperature experiments using the multi-anvil press (MAP) in the high pressure lab at NASA-JSC. Multiple MAP experiments were conducted and analytical results from three of these experiments are reported here.

The experiments (GN10, GN11, and GN13) were conducted using standard COMPRES assemblies. All were in MgO capsules. Both GN10 and GN11 used 8/3 assemblies and GN13 a 10/5 assembly. The experimental run temperatures were all approximately 2200°C though peak temperatures were slightly higher. These temperatures are above the peridotite solidus, which is the appropriate temperature for metal-silicate segregation in the Earth⁹. Pressures were: GN10, 26 GPa; GN11, 23 GPa; and GN13, 18 GPa. These pressures

were determined from calibrations run at approximately 1400°C, therefore the actual pressures at peak run temperatures may be lower. The paucity of silicate perovskite in the two higher P runs suggests that experimental pressures at peak T may have been 2 to 3 GPa lower than the reported values (see Discussion).

Starting materials for all three experiments consisted of a mixture of peridotite and metal powders with an approximate 2:1 wt% silicate to metal ratio. The peridotite is spinel lherzolite from xenoliths collected in Hannouba, China and provided by Dr. R. Rudnick (UMd).¹¹ The metals consist of Fe and W in a ratio of approximately 5:1 wt% with minor Mo (<1 wt%).

Run-products were analyzed using electron microprobes at both NASA-JSC (Cameca SX-100) and UMD (JEOL JXA-8900R). Figure 1 shows a typical run product. Mineral phases in this sample include wadsleyite, majorite, Ca-majorite, and silicate perovskite.

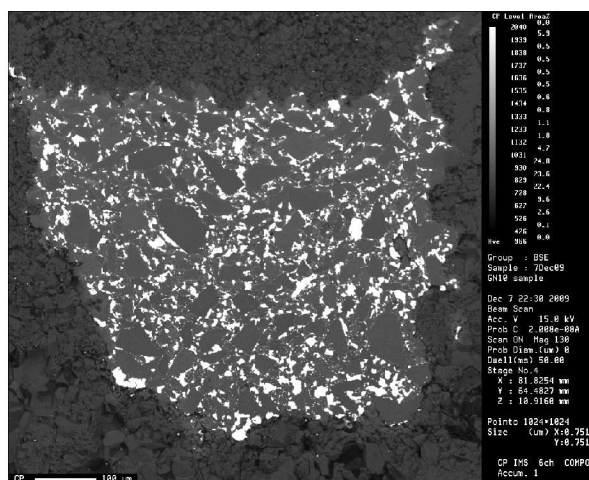


Figure 1. BSE image of run product GN10, P=26 GPa and T=2200°C.

Discussion: None of the silicate melt quenched to a glass, hence the texture of all run products is crystalline, which is typical of melting experiments using peridotite starting materials. The silicate fraction is characterized by a combination of fairly large grains (20 to 50 microns) and smaller grains (10 to 20 microns). Interstitial quenched melt regions are present and are comprised of fine-grained aggregates of crystals typically less than five microns along their longest dimension with many grains on the order of 1-2 microns.

The larger crystals are mostly homogeneous though small inclusions of other phases are observed.

Mineral phase identifications were made by stoichiometry, guided by the P-T conditions of the experiments and referenced to published phase diagrams¹². The silicate mineral phases are wadsleyite, majorite, Ca-majorite, ferropericlasite, and akimotoite. One grain of probable silicate perovskite was observed in each of the higher pressure runs (GN10 and GN11).

All metal grains in the samples are assemblages of two distinct phases. The textures range from lamellar to equigranular. These two phases are identifiable in BSE image based on contrast. The major phase across all three samples has an average composition of 83 wt% Fe and 14 wt% W, and the minor exsolved phase 70 wt% Fe and 27 wt% W. The remaining 3% are in Ni, Cr, and Mo. The exsolved phase comprises approximately 10% of the metal volume. Volume-averaged metal compositions were calculated for the partition coefficient computations of each sample.

Liquid metal/solid silicate partition coefficients (D_W) were calculated for each silicate mineral phase from data for each sample run product. Liquid metal/liquid silicate coefficients were calculated for the identified melt regions of the two lower P runs, GN11 and GN13, labeled 'Melt' in Figure 2. Oxygen fugacities were determined from the compositions of ferropericlasite and coexisting metal, assuming ideal solutions. In Figure 2, all D_W were corrected to IW-2 fO₂ conditions to allow a more meaningful comparison of D_W values between phases and experiments and for comparison to published partitioning data. Other published data is shown from experiments conducted using a range of both silicate compositions and temperatures^{3,4,8,13,14,15,16}.

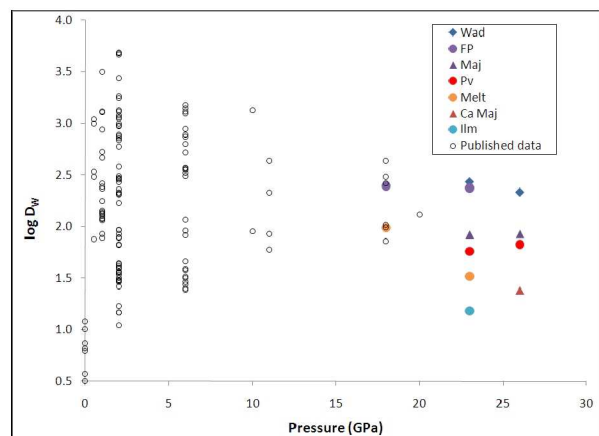


Figure 2. Plot of $\log D_W$ vs. pressure for W. D_W values from our experiments are metal/mineral coefficients. Uncertainties on D_W range from 8% to 24%. Published data are shown for comparison.

The present data suggest that the effect of higher-pressure (>10 GPa) on W partitioning is slight as shown by the nearly horizontal trend of the data. This is in accord with the interpretations of other authors^{5,8}.

However, the current data set, including our experiments, still extend only to the mid-20 GPa range and the trajectory of W partitioning to pressures higher than approximately 26 GPa remains weakly constrained by experiments. It has been shown that predictions of high pressure behavior can fail to capture the actual behavior shown by experimental evidence, and therefore metal-silicate partitioning data at yet higher pressures will be an important addition to this discussion^{17,18}.

References: [1] Righter, K. & Drake, M.J. (1996) *Icarus* 124, 513-529, [2] Halliday, A.N. (2003) in Davis (ed.) *Meteorites, Comets and Planets: Treatise on Geochemistry*, 509-557, [3] Walter, M.J. & Thibault, Y. (1995) *Science* 270, 1186-1189, [4] Hillgren, V.J., et al. (1996) *Geochim.* 60, 2257-2263, [5] Righter, K., et al., (1997) *EPSL* 100, 115,134, [6] O'Neill H.St.C., et al., (2008) *Chem Geol* 255, 346-359, [7] Ohtani, E., et al., (1997) *Phys Earth Planet Int* 100, 97-114, [8] Cottrell, E., et al., (2009) *EPSL* 281, 275-287, [9] Wade, J., & Wood, B.J. (2005) *EPSL* 236, 78-95, [10] Li, J., & Agee, C.B. (1996) *Nature* 381, 686-689, [11] Rudnick, R., et al., (2004) *Lithos* 77, 609-637, [12] Gasparik, T. (2003) in *Phase diagrams for geoscientists: an atlas of the Earth's interior*, Springer-Verlag, Berlin, [13] Newsom, H.E. & Drake, M.J. (1982) *Geochim* 46, 2483-2489, [14] Jaeger, W.L. & Drake, M.J. (2000) *Geochim* 64, 3887-3895, [15] Righter, K. & Drake, M.J. (1999) *EPSL* 171, 383-399, [16] Shearer, C.K. & Righter, K. (2003) *GRL* 30, 1007-1-1007-4 [17] Tschauner et al, (1999) *Nature* 398, 604-607, [18] Campbell et al., (2009) *EPSL* 286, 556-564.